Highly entangled photons and rapidly responding polarization qubit phase gates in a room-temperature active Raman gain medium

Chao Hang[1,2] and Guoxiang Huang[1,3,*]
[1] *State Key Laboratory of Precision Spectroscopy and Department of Physics, East China Normal University, Shanghai 200062, China*
[2] *Centro de Física Teórica e Computacional, Universidade de Lisbon, Complex Interdisciplinary, Avenida Professor Gama Pinto 2, Lisbon P-1649-003, Portugal*
[3] *Institute of Nonlinear Physics, Zhejiang Normal University, Jinhua, Zhejiang 321004, China*
(Received 5 September 2010; published 16 November 2010)

We present a scheme for obtaining entangled photons and quantum phase gates in a room-temperature four-state tripod-type atomic system with two-mode active Raman gain (ARG). We analyze the linear and nonlinear optical responses of this ARG system and show that the scheme is fundamentally different from those based on electromagnetically induced transparency and hence can avoid significant probe-field absorption as well as a temperature-related Doppler effect. We demonstrate that highly entangled photon pairs can be produced and rapidly responding polarization qubit phase gates can be constructed based on the unique features of the enhanced cross-phase-modulation and superluminal probe-field propagation of the system.

DOI: 10.1103/PhysRevA.82.053818 PACS number(s): 42.65.Dr, 42.50.Gy, 03.67.Bg

I. INTRODUCTION

Efficient schemes for producing entangled photons and constructing all-optical quantum gates are very important in optical quantum-information processing and computation [1]. Toward this end, a significant suppression of optical absorption and a giant enhancement of Kerr nonlinearity are crucial. However, in a conventional medium this cannot be efficiently implemented because optical fields far away from atomic resonance are used to avoid large optical absorption, and hence the Kerr nonlinearity of the system is usually very weak.

In recent years, much attention has been paid to the study of electromagnetically induced transparency (EIT) in resonant atomic systems [2,3]. The wave propagation in EIT media possesses many striking features, such as the large suppression of optical absorption, the significant reduction of group velocity, and the giant enhancement of Kerr nonlinearity [2]. Based on these features, many EIT-based applications, including optical quantum memory [4], highly efficient multi-wave mixing [2], optical atomic clocks [5–7], and slow-light solitons [8–11], have been studied intensively. Moreover, EIT-based schemes for producing entangled photons [12–14] and polarization qubit quantum phase gates (QPGs) [15–18] have also been proposed. However, the EIT-based schemes have some inherent drawbacks, such as the probe attenuation and spreading at room temperature and the long response time due to the nature of ultraslow propagation [19]. These drawbacks impede the potential applications of EIT media for rapidly responding all-optical devices at room temperature.

In this work, we propose a scheme to realize highly efficient entangled photons and rapidly responding polarization QPGs in a resonant atomic system. The scheme is based on active Raman gain (ARG) (or gain-assisted) configurations, which were demonstrated to be able to produce stable superluminal propagations of optical waves [20–25]. Contrary to the EIT-based schemes in which the probe field operates in an absorption mode, the key idea of the ARG-based scheme is that the probe field operates in a stimulated Raman emission mode. Therefore, the ARG-based scheme can avoid being affected by a temperature-related Doppler effect and significant probe-field attenuation or distortion. Recently, it was shown by Deng *et al.* [26,27] that large and rapidly responding cross-Kerr effects are possible in ARG-based media. In addition, superluminal optical solitons are also predicted in such systems [28,29]. The system we suggest here is a four-state tripod-type atomic system with a two-mode pump field and two weak fields. We prove that the unique features of the present system can be used to produce highly entangled photon pairs and implement rapidly responding polarization QPGs. Contrary to the entangled photons and QPGs in EIT media [15–18], the present ARG scheme has the following advantages: (i) It is able to eliminate the significant probe attenuation and distortion induced by a temperature-related Doppler effect, and hence we can produce highly entangled photons and implement QPGs with high reliability at room temperature. (ii) It allows superluminal wave propagation, and hence one can implement QPGs with a very rapid response. The results presented in this work may be useful for guiding related experiments and facilitating practical applications in quantum-information science [30].

The paper is organized as follows. In the next section, we give a description of the model under study and present the expressions of electric susceptibilities and the group velocity of the probe and signal fields. In Sec. III, we describe a method to produce entangled superluminal photons and construct polarization QPGs based on the present ARG system. In the final section, we provide a simple discussion on temperature-related Doppler effect and quantum noise. The main results of our research are also summarized.

II. THE MODEL AND LINEAR AND NONLINEAR SUSCEPTIBILITIES

We start by considering a lifetime-broadened four-level tripod-type atomic gas interacting with a strong continuous-wave two-mode pump laser field (with electric fields E_{P1} and E_{P2}) and two weak, pulsed laser (probe and signal) fields (with electric fields E_p and E_s), as shown in Fig. 1. The pump fields E_{P1} and E_{P2} are of π polarization and couple the ground state

*gxhuang@phy.ecnu.edu.cn

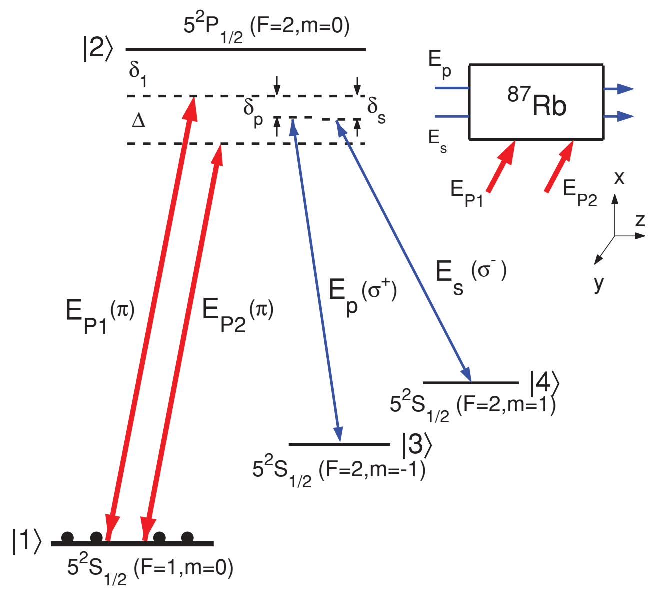

FIG. 1. (Color online) The energy levels $|l\rangle$ ($l = 1$–4) and excitation scheme of the lifetime-broadened four-state tripod-type atomic system interacting with a strong continuous-wave two-mode pump laser field (with electric fields E_{P1} and E_{P2}) and two weak, pulsed (probe and signal) fields (with electric fields E_p and E_s). E_{P1} and E_{P2} are of π polarization, while E_p (E_s) is of σ^+ (σ^-) polarization, and δ_1, δ_p, δ_s, and Δ are detunings. The inset shows the possible geometry of the experimental set.

$|1\rangle$ to the excited state $|2\rangle$ with large one-photon detunings δ_1 and $\delta_1 + \Delta$ ($|\Delta| \ll |\delta_1|$), respectively. The probe (signal) field E_p (E_s) is of σ^+ (σ^-) polarization and couples the excited state $|2\rangle$ to the hyperfine state $|3\rangle$ ($|4\rangle$) with a two-photon detuning δ_p (δ_s). The system contains two Raman resonances due to the two-mode pump field for each weak field. Our scheme can be realized by a specific implementation using the D_1 line of ^{87}Rb, where a homogeneous magnetic field parallel to the laser propagation direction is applied to encode binary information and avoid the undesirable couplings. A possible geometry of experimental arrangement is suggested in the inset of the figure. Note that the system we are considering here is a direct extension (by adding a new, weak signal field) of that used by Wang *et al.* [22] for the remarkable observation of stable, superluminal light propagation in an ARG system.

The evolution equations for the atomic probability amplitudes $a_l(t)$ ($l = 1$–4) are

$$\dot{a}_1 = \frac{\gamma_1}{2}a_1 + i\Omega_{P1}^* e^{i\delta_1 t} a_2 + i\Omega_{P2}^* e^{i(\delta_1+\Delta)t} a_2, \quad \text{(1a)}$$

$$\dot{a}_2 = -\frac{\gamma_2}{2}a_2 + i\Omega_{P1} e^{-i\delta_1 t} a_1 + i\Omega_{P2} e^{-i(\delta_1+\Delta)t} a_1 + i\Omega_p e^{-i(\delta_1+\delta_p)t} a_3 + i\Omega_s e^{-i(\delta_1+\delta_s)t} a_4, \quad \text{(1b)}$$

$$\dot{a}_3 = -\frac{\gamma_3}{2}a_3 + i\Omega_p^* e^{i(\delta_1+\delta_p)t} a_2, \quad \text{(1c)}$$

$$\dot{a}_4 = -\frac{\gamma_4}{2}a_4 + i\Omega_s^* e^{i(\delta_1+\delta_s)t} a_2, \quad \text{(1d)}$$

where $\Omega_{Pn} = -D_{21}\mathcal{E}_{Pn}/(2\hbar)$ ($n = 1,2$), $\Omega_p = -D_{23}\mathcal{E}_p/(2\hbar)$, and $\Omega_s = -D_{24}\mathcal{E}_s/(2\hbar)$ are half-Rabi frequencies for $|1\rangle \leftrightarrow |2\rangle$, $|3\rangle \leftrightarrow |2\rangle$, and $|4\rangle \leftrightarrow |2\rangle$ transitions, with relevant electric-dipole moments D_{21}, D_{23}, and D_{24} and electric-field envelopes $\mathcal{E}_{Pn}$, $\mathcal{E}_p$, and $\mathcal{E}_s$, respectively. The detunings are defined by $\delta_1 = \omega_{21} - \omega_{P1}$, $\Delta = \omega_{21} - \omega_{P2} - \delta_1$, $\delta_p = \omega_{23} - \omega_p - \delta_1$, and $\delta_s = \omega_{23} - \omega_s - \delta_1$ (see Fig. 1). The variable γ_1 denotes the gain of state $|1\rangle$ for describing the effect of atoms going back to the ground state before being excited again, and γ_l ($l = 2$–4) denotes the decay rates of state $|l\rangle$ for describing the effects of both spontaneous emission and dephasing. In the present work, we are interested in a closed system, that is, there is no decay to levels outside the system we study, and hence γ_1 can be determined by the decay rates of higher states γ_l ($l = 2$–4) through the conservation of particle number $\sum_{l=1}^4 |a_l|^2 = 1$ [see Eq. (3)]. Notice that here we employ the amplitude variable approach for the description of the motion of atoms, and γ_l is introduced in a phenomenological manner. A complete description including spontaneous emission and dephasing can be obtained by a density-matrix equation approach. However, for the ARG-based coherent atomic systems, two approaches are equivalent.

In order to investigate the propagation of the probe and signal fields, Eqs. (1) must be solved simultaneously with the Maxwell equation. With the electric field defined by $E_j = \mathcal{E}_j \exp[i(k_j - \omega_j t)]$ + c.c., we obtain

$$i\left(\frac{\partial}{\partial z} + \frac{1}{v_g^j}\frac{\partial}{\partial t}\right)\mathcal{E}_j + \frac{\omega_j}{2c}\chi_j\mathcal{E}_j = 0 \quad (j = p, s) \quad \text{(2)}$$

under the slowly varying amplitude approximation, where v_g^j is the group velocity, generally defined as $v_g^j = c/(1 + n_g^j)$, with $n_g^j = \mathrm{Re}(\chi_j)/2 + (\omega_j/2)[\partial\,\mathrm{Re}(\chi_j)/\partial\omega]|_{\omega=\omega_j}$ being the group index. The susceptibilities of the two weak fields are defined by $\chi_{p,s} = \mathcal{N}_a D_0 a_2 a_{3,4}^*/(\epsilon_0\mathcal{E}_{p,s})$ ($D_{23} \simeq D_{24} = D_0$), where $\mathcal{N}_a$ is the atomic concentration.

We assume that atoms are initially populated in the ground state $|1\rangle$. For large one-photon detunings δ_1 and $\delta_1 + \Delta$, the ground-state depletion is not significant, that is, $a_1 \simeq 1$. However, in order to take into account the nonlinear effect, we need to consider the higher-order contribution of a_1, which can be obtained by using the condition $\sum_{i=1}^4 |a_i|^2 = 1$. Meanwhile, we assume that the typical temporal duration of the probe and signal fields is long enough so that we can solve the equations adiabatically. With these considerations, we obtain the expressions of γ_1 and the electric susceptibilities of the system,

$$\gamma_1 = \gamma_2(G_1 + G_2) + \gamma\left(\frac{G_1}{\delta_2^2} + \frac{G_2}{(\delta_2 - \Delta)^2}\right)\times(|\Omega_p|^2 + |\Omega_s|^2) \quad \text{(3)}$$

and

$$\chi(\omega_j) \simeq \chi_j^{(1)} + \chi_j^{(3,s)}|\mathcal{E}_j|^2 + \chi_j^{(3,c)}|\mathcal{E}_{j'}|^2, \quad \text{(4)}$$

with $j, j' = p, s$ ($j \neq j'$), and

$$\chi_j^{(1)} \simeq -\kappa\left(\frac{G_1}{\delta_2 - i\gamma/2} + \frac{G_2}{\delta_2 - \Delta - i\gamma/2}\right), \quad \text{(5a)}$$

$$\chi_j^{(3,s)} = \chi_j^{(3,c)} \simeq \kappa'\left(\frac{G_1}{\delta_2 - i\gamma/2} + \frac{G_2}{\delta_2 - \Delta - i\gamma/2}\right) \times\left(\frac{G_1}{\delta_2^2} + \frac{G_2}{(\delta_2 - \Delta)^2}\right). \quad \text{(5b)}$$

Here, $\chi_j^{(1)}$, $\chi_j^{(3,s)}$, and $\chi_j^{(3,c)}$ determine the linear, self-, and cross-Kerr nonlinear responses of the system. The constants in (3) and (5) are defined by $G_1 = |\Omega_{P1}|^2/\delta_1^2$, $G_2 = |\Omega_{P2}|^2/(\delta_1+\Delta)^2$, $\kappa = \mathcal{N}_a|D_2|^2/(\hbar\epsilon_0)$, and $\kappa' = \mathcal{N}_a|D_2|^4/(\hbar^3\epsilon_0)$. We should also mention that in order to obtain simplified expressions of γ_1 [i.e., Eq. (3)] and third-order susceptibility [i.e., Eq. (5b)], we have taken $\delta_p = \delta_s = \delta_2$ and $\gamma_3 \simeq \gamma_4 = \gamma$ and used the conditions $\gamma_2^2 \ll \delta_1^2$, $\gamma^2 \ll \delta_2^2$, $\gamma^2 \ll (\delta_2 - \Delta)^2$, and $G_{1,2} \ll 1$. The real and imaginary parts of $\chi_j^{(1)}$ denote the phase shift per unit length and absorption or gain, respectively. From the expression of Eq. (5b), we see that the linear susceptibility for both the probe and signal fields has two Raman resonances, which contribute from two pump fields. If $\delta_2 = \Delta/2$ and the intensities of the two pump fields are well adjusted so that $G_1 = G_2 = G$, one has $\mathrm{Re}(\chi_j^{(1)}) = 0$, and hence a gain-dependent linear phase can be completely removed [26]. In this case, $2\,\mathrm{Im}(\chi_j^{(1)}) \simeq -8\kappa G\gamma/\Delta^2$ describes the intensity gain acquired by two weak fields. This is fundamentally different from all EIT-based systems, which are inherently absorptive. The previous choice of two-mode pump intensities and two-photon detuning also yields $\mathrm{Re}(\chi_j^{(3)}) = 0$ and $2\mathrm{Im}(\chi_j^{(3)}) \simeq 64\kappa' G^2\gamma/\Delta^4$, that is, a zero nonlinear phase shift and a nonzero nonlinear intensity absorption. Therefore, in order to obtain a nonzero nonlinear phase shift, we need to slightly disturb the conditions $\delta_2 = \Delta/2$ or $G_1 = G_2 = G$.

In Fig. 2, we show the results of direct simulations of Eqs. (1) with a set of practical parameters given in the caption. The initial conditions are $a_1 = 1$ and $a_2 = a_3 = a_4 = 0$. The dependence of atomic probability amplitudes a_l ($l = 1$–4) and quantity $\sum_{i=1}^4 |a_i|^2$ on time are illustrated. We can see that the condition $\sum_{i=1}^4 |a_i|^2 = 1$ is satisfied in a rather long time.

In Fig. 3(a) [Fig. 3(b)], we show the curves of $\mathrm{Re}(\chi_j^{(1)})$ $[-\mathrm{Im}(\chi_j^{(1)})]$ and $\mathrm{Re}(\chi_j^{(3)})$ $[-\mathrm{Im}(\chi_j^{(3)})]$ versus δ_2 with a set of practical parameters given in the caption [31]. A gain doublet structure in the spectrum can be apparently observed [see panel (b)], where a gain minimum can be acquired at $\delta_2 = \Delta/2$. Thus, when working near the gain minimum within the hole, a rapid increase of light intensity appearing in the ARG system can be effectively avoided. In Fig. 3(c), we show the curves of v_g^j/c versus δ_2. The group velocity is negative (with a small absolute value) corresponding to the superluminal propagation.

Now we present the expressions of group velocities for both weak fields, which are defined by $v_g^j = c/(1+n_g^j)$ $(j = p,s)$. As we know, the group velocities of two light pulses must be comparable in order to achieve an effective cross-phase-modulation (CPM) [12]. In our system, the group indexes of the probe and signal fields are given by

$$n_g^j \simeq -\frac{\kappa\omega_j}{2}\left(\frac{G_1}{\delta_2^2} + \frac{G_2}{(\delta_2-\Delta)^2}\right). \tag{6}$$

Because in our system $\omega_p \approx \omega_s$, we have $v_g^p \approx v_g^s$, and hence the group-velocity matching is automatically satisfied. In addition, since $n_g^j \ll -1$ (due to the large values of ω_j), both group velocities are negative; that is, the probe and signal fields travel with superluminal propagating velocities.

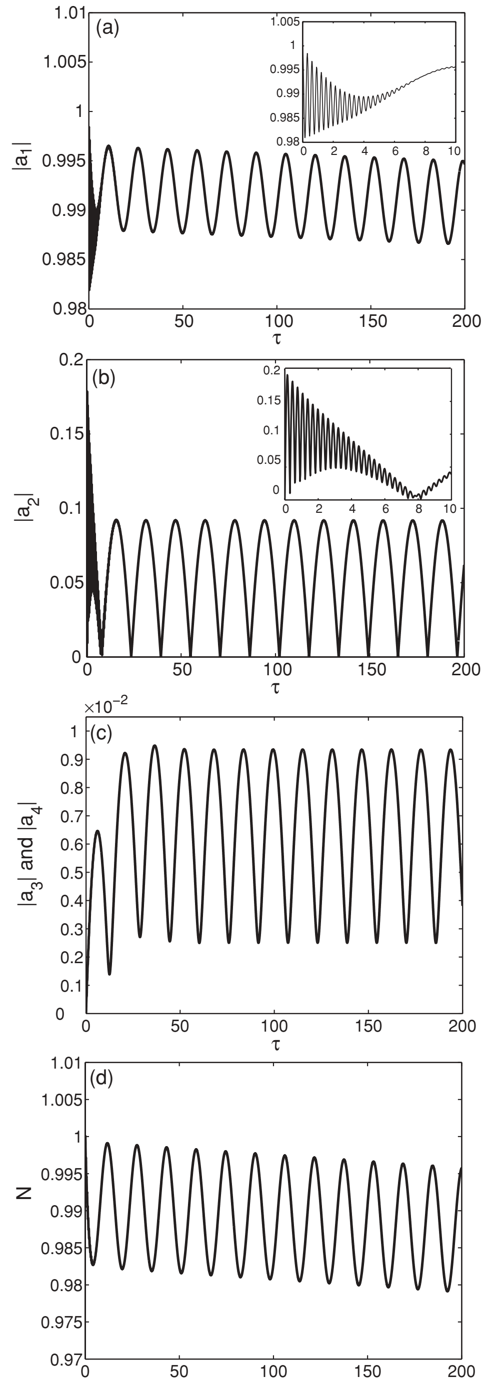

FIG. 2. The results of direct simulations of Eqs. (1) with the initial conditions $a_1 = 1$ and $a_2 = a_3 = a_4 = 0$. (a) The curves of $|a_1|$ vs τ. The inset shows the details for $\tau \in [0,10]$. (b) The curves of $|a_2|$ vs τ. The inset shows the details for $\tau \in [0,10]$. (c) The curves of $|a_j|$ $(j = 3,4)$ vs τ. (d) The curves of N vs τ. Here, $N \equiv \sum_{i=1}^4 |a_i|^2$ and $\tau \equiv \Omega_{P1}t$. The parameters are given by $\gamma_2 = 36$ MHz, $\gamma = 10$ MHz, $\delta_1 = 1.0 \times 10^9$ s^{-1}, $\delta_2 = 1.0 \times 10^7$ s^{-1}, $\Delta = 2.0 \times 10^7$ s^{-1}, $\Omega_{P1} = 5.0 \times 10^7$ s^{-1}, $\Omega_{P2} = 5.1 \times 10^7$ s^{-1}, and $\Omega_p = \Omega_s = 1.0 \times 10^6$ s^{-1}. The value $\gamma_1 = 0.2$ MHz is obtained by Eq. (3).

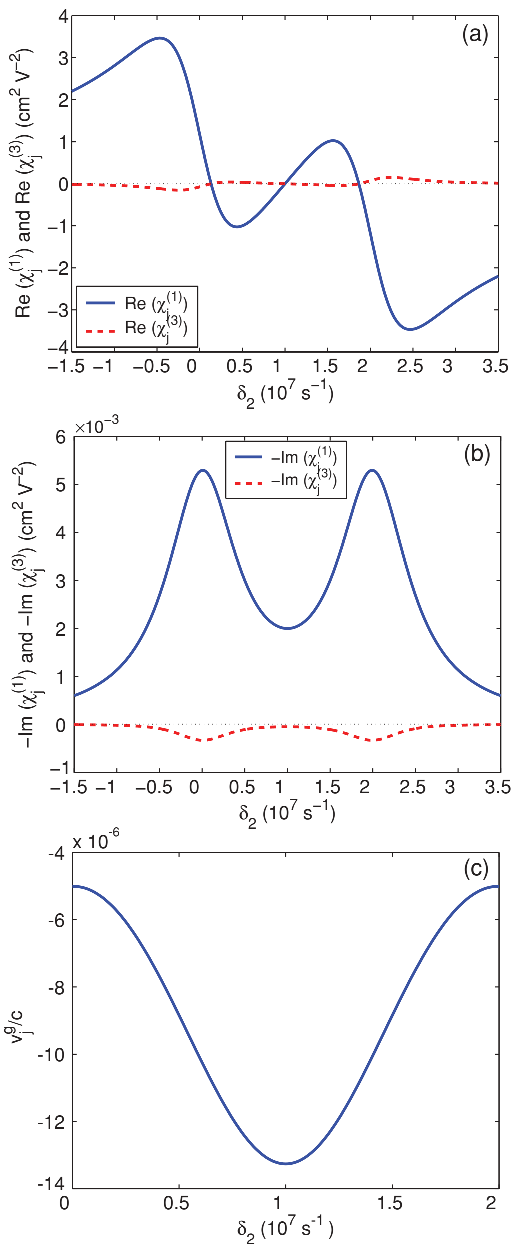

FIG. 3. (Color online) (a) The curves of $\mathrm{Re}(\chi_j^{(1)})$ (solid line) and $\mathrm{Re}(\chi_j^{(3)})$ (dashed line) vs δ_2. (b) The curves of $-\mathrm{Im}(\chi_j^{(1)})$ (solid line) and $-\mathrm{Im}(\chi_j^{(3)})$ (dashed line) vs δ_2. (c) The curve of v_g^j/c vs δ_2. The parameters are given by $\gamma_2 = 36$ MHz, $\gamma = 10$ MHz, $\delta_1 = 1.0 \times 10^9\ \mathrm{s}^{-1}$, $\Delta = 2.0 \times 10^7\ \mathrm{s}^{-1}$, $\Omega_{P1} = 5.0 \times 10^7\ \mathrm{s}^{-1}$, $\Omega_{P2} = 5.1 \times 10^7\ \mathrm{s}^{-1}$, $\mathcal{N}_a = 1.44 \times 10^{13}\ \mathrm{cm}^{-3}$, and $D_0 = 2.54 \times 10^{-27}$ C cm.

III. TWO-QUBIT POLARIZATION PHASE GATES AND HIGHLY ENTANGLED PHOTONS

The prototype of optical implementation of a two-qubit gate is the QPG in which one qubit gets a phase shift conditional to the other qubit state according to the transformation $|i\rangle_1|j\rangle_2 \to \phi_{ij}|i\rangle_1|j\rangle_2$, where $i,j = 0,1$ denote logical qubit bases. This gate becomes universal when $\phi_{11} + \phi_{00} - \phi_{10} - \phi_{01} \neq 0$ [32].

We choose two orthogonal polarization states $|\sigma^-\rangle$ and $|\sigma^+\rangle$ to encode binary information for each qubit. The scheme shown in Fig. 1 is completely implemented only if both probe and signal fields have the "right" polarization states. When both of the two weak fields have the "wrong" polarization states, there is no sufficiently close excited state to which levels $|3\rangle$ and $|4\rangle$ can couple, and hence the probe and signal fields will only acquire the trivial vacuum phase shift $\phi_0^j = k_j L$. Here $k_j \equiv \omega_j/c$ $(j = p,s)$, and L denotes the length of the medium. When one of the two weak fields has the "wrong" polarization state, say for a σ^--polarized probe field, there is no sufficiently close excited state to which levels $|3\rangle$ can couple, and the signal field is subjected to the Λ configuration constituted by the $|1\rangle$, $|2\rangle$, and $|4\rangle$ levels. Thus the signal field experiences a self-Kerr effect and acquires a nontrivial phase shift ϕ_1^s, while the probe field acquires only a vacuum phase shift ϕ_0^p. When only the probe and the signal fields have the "right" polarization states, they all acquire nontrivial phase shifts ϕ_2^p and ϕ_2^s, respectively.

Assume that the input probe and signal pulses can be treated as polarized single-photon wave packets, expressed as a superposition of the circularly polarized states, that is, $|\psi\rangle_j = (1/\sqrt{2})|\sigma^-\rangle_j + (1/\sqrt{2})|\sigma^+\rangle_j$ $(j = p,s)$. Here $|\sigma^\pm\rangle_j = \int d\omega \xi_j(\omega) a_\pm^\dagger(\omega)|0\rangle$, with $\xi_j(\omega)$ being a Gaussian frequency distribution of incident wave packet centered at frequency ω_j. The photon field operators undergo a transformation while propagating through the atomic medium of length L, that is, $a_\pm(\omega) \to a_\pm(\omega)\exp\{(i\omega/c)\int_0^L dz n_\pm(\omega,z)\}$. Assuming $n_\pm(\omega,z)$ (the real part of the refractive index) varies slowly over the bandwidth of the wave packet centered at ω_j, one gets $|\sigma^\pm\rangle_j \to \exp(-i\phi_\pm^j)|\sigma^\pm\rangle_j$, with $\phi_\pm^j = \omega_j n_\pm(\omega_j,z)L/c$. Thus, the truth table for a polarization two-qubit QPG using the present configuration is given by

$$|\sigma^-\rangle_p|\sigma^+\rangle_s \to \exp\left[-i\left(\phi_0^p + \phi_0^s\right)\right]|\sigma^-\rangle_p|\sigma^+\rangle_s, \tag{7a}$$
$$|\sigma^-\rangle_p|\sigma^-\rangle_s \to \exp\left[-i\left(\phi_0^p + \phi_1^s\right)\right]|\sigma^-\rangle_p|\sigma^-\rangle_s, \tag{7b}$$
$$|\sigma^+\rangle_p|\sigma^+\rangle_s \to \exp\left[-i\left(\phi_1^p + \phi_0^s\right)\right]|\sigma^+\rangle_p|\sigma^+\rangle_s, \tag{7c}$$
$$|\sigma^+\rangle_p|\sigma^-\rangle_s \to \exp\left[-i\left(\phi_2^p + \phi_2^s\right)\right]|\sigma^+\rangle_p|\sigma^-\rangle_s, \tag{7d}$$

where $\phi_0^j = k_j L$, $\phi_1^j = k_j L(1 + 2\pi\chi_j^{(1)}) + \phi^{(j,s)}$, and $\phi_2^j = \phi_1^j + \phi^{(j,c)}$, with

$$\phi^{(j,s)} = k_j L \frac{\pi^{3/2}\hbar^2|\Omega_j|^2}{4|D_2|^2}\mathrm{Re}\left(\chi_j^{(3,s)}\right), \tag{8a}$$
$$\phi^{(j,c)} = k_j L \frac{\pi^{3/2}\hbar^2|\Omega_{j'}|^2}{4|D_2|^2}\mathrm{Re}\left(\chi_j^{(3,c)}\right)\frac{\mathrm{erf}(\xi_{jj'})}{\xi_{jj'}}, \tag{8b}$$

contributed, respectively, by self-phase-modulation (SPM) and CPM, where $\xi_{jj'} = \sqrt{2}L(1 - v_g^j/v_g^{j'})/(\tau_{j'}v_g^j)$, with $\tau_{j'}$ being the width of the pulse. If group-velocity matching is satisfied, that is, $\xi_{jj'} \to 0$, $\mathrm{erf}(\xi_{jj'})/\xi_{jj'}$ reaches its maximum value $2/\sqrt{\pi}$.

From Eq. (7), we can compute the degree of entanglement of the two-qubit state by using the entanglement of formation. For an arbitrary two-qubit system, it is given by [33]

$$E_F(C) = h\left(\frac{1 + \sqrt{1 - C^2}}{2}\right), \tag{9}$$

where $h(x) = -x\log_2(x) - (1 - x)\log_2(1 - x)$ is Shannon's entropy function and C is the concurrence given by

$C(\hat{\rho}) = \max\{0,\lambda_1 - \lambda_2 - \lambda_3 - \lambda_4\}$. Here λ_i's are square roots of eigenvalues of the matrix

$$\hat{\rho}\tilde{\hat{\rho}} = \hat{\rho}\hat{\sigma}_y^p \otimes \hat{\sigma}_y^s \hat{\rho}^* \hat{\sigma}_y^p \otimes \hat{\sigma}_y^s \tag{10}$$

in decreasing order. The density matrix $\hat{\rho}$ in Eq. (10) can be directly obtained by using Eq. (7), the quantity $\tilde{\hat{\rho}}$ ($\hat{\rho}^*$) denotes the transpose (complex conjugation) of $\hat{\rho}$, and $\hat{\sigma}_y$ denotes the y component of the Pauli matrix.

Equation (7) supports a universal QPG if the conditional phase shift [32]

$$\begin{aligned}(\phi_0^p + \phi_0^s) + (\phi_2^p + \phi_2^s) - (\phi_0^p + \phi_1^s) - (\phi_1^p + \phi_0^s)\\ = \phi^{(p,c)} + \phi^{(s,c)}\end{aligned} \tag{11}$$

is nonzero. From this formula, we see that only the phase shifts due to the CPM effect contribute to the conditional phase shifts.

Now we provide a practical set of parameters corresponding to typical values of ^{87}Rb atoms at room temperature. The decay rate of the lower states, that is, $|3\rangle$ ($5^2S_{1/2}$, $F = 2, m = -1$) and $|4\rangle$ ($5^2S_{1/2}$, $F = 2, m = 1$), is $\gamma = 300$ Hz. The hyperfine splitting between the lower states can be adjusted by the intensity of an externally applied magnetic field. For a magnetic field ≈340 G, we obtain the splitting ≈3.8 GHz. The decay rate of the higher state $|2\rangle$ ($5^2P_{1/2}$, $F = 2, m = 0$) is $\gamma_2 = 36$ MHz. The other parameters are taken the same as those used in Fig. 2, as well as $\delta_2 = 0.8 \times 10^7$ s^{-1}. With the given parameters, we obtain that $\chi_j^{(1)} = -0.10 \times 10^{-2} - i0.85 \times 10^{-7}$ and $\chi_j^{(3)} = 0.34 \times 10^{-4} + i0.28 \times 10^{-8}$ cm^2 V^{-2}. We note that the imaginary parts of the susceptibilities are much smaller than those of the real parts due to the conditions $\gamma_2 \ll \delta_1$, $\gamma \ll \delta_2$, and $\delta_2 \neq \Delta/2$. A very small total gain effect remains after the balance of the linear gain and nonlinear absorption. The real parts of the third-order susceptibilities are about $\sim 10^{13}$ times larger than those measured for usual nonlinear optical materials, that is, a giant enhancement of CPM can be achieved in our system. The group velocities of both the probe and signal fields are very well matched, with the values

$$v_g^p \approx v_g^s = -0.94 \times 10^{-5} c \tag{12}$$

corresponding to a superluminal propagation.

In Fig. 4(a), we calculated the result of the degree of entanglement versus the propagation of the device length L. We see that a nearly 100% degree of entanglement can be obtained at $L = 0.53$ cm. The reason for acquiring such a high degree of entanglement is due to the nonabsorption feature of the system. Shown in Fig. 4(b) are the curves of CPM-induced phase shifts $\phi^{(p,c)}$ and $\phi^{(s,c)}$ versus L. We see that a conditional phase shift $\phi^{(p,c)} + \phi^{(s,c)}$ up to π radians can be obtained at $L \simeq 0.53$ cm, corresponding to the point of the maximum entanglement in Fig. 4(a). In Fig. 4(c), we show the curves of $\phi^{(p,c)}$ and $\phi^{(s,c)}$ versus δ_2 at $L = 0.53$ cm.

The probe and signal fields can have a mean amplitude of about one photon when these beams are focused or propagate in a tightly confined waveguide (e.g., hollow-core photonic crystal fibers [34]). With these parameters, we obtain the intensities of the probe (I_p) and signal (I_s) fields, given by $I_p \approx I_s = 0.23 \times 10^{-6}$ W cm^{-2} when $\Omega_p \approx \Omega_s = 1.0 \times 10^6$ s^{-1}. We remark that the intensity of a single 800-nm photon per nanosecond on the area of 1 μm^2 is $I_{\rm ph} = 2.5 \times 10^{-2}$ W cm^{-2}.

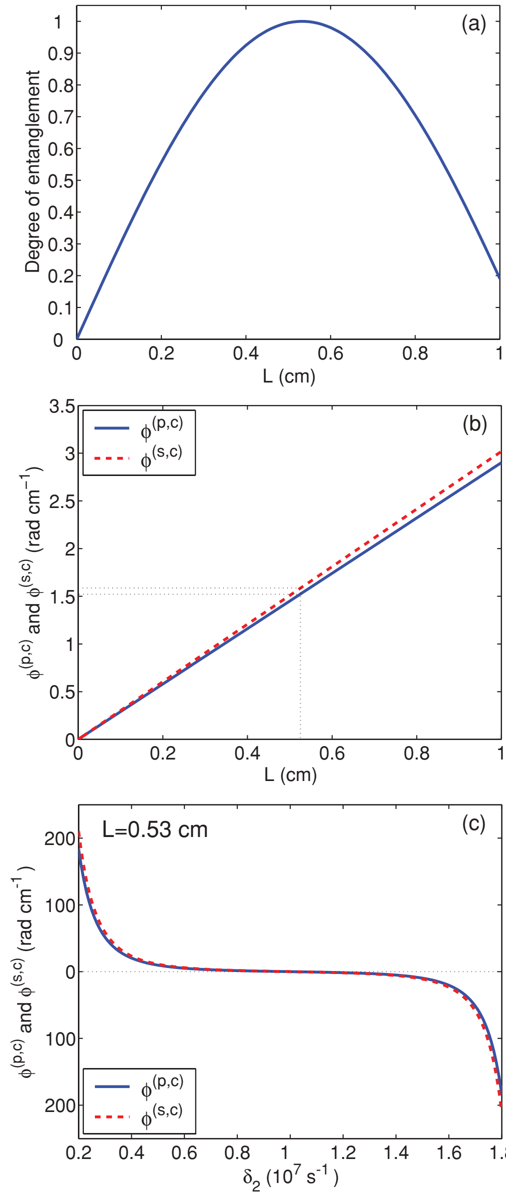

FIG. 4. (Color online) (a) The degree of entanglement vs the device length L. (b) The curves of $\phi^{(p,c)}$ and $\phi^{(s,c)}$ vs L. A conditional phase shift $\phi^{(p,c)} + \phi^{(s,c)}$ up to π radians can be obtained at $L \simeq 0.53$ cm. (c) The curves of $\phi^{(p,c)}$ and $\phi^{(s,c)}$ vs δ_2 at $L = 0.53$ cm. The parameters are given in the text.

This shows that our scheme can indeed make a polarization QPG with a π-conditional phase shift possible with single-photon wave packets. Based on the superluminal propagating velocities and the enhanced CPM, the probe and signal fields acquire nontrivial nonlinear phase shifts when both of them have the "right" polarization states in a fast response time and a short propagation distance. This allows us to implement a rapidly responding phase gate. For instance, if the group velocity of the probe and signal waves is reduced $10^{-4}c$ when using the EIT-based scheme, these waves will take around 180 ns to pass the device (for $L = 0.53$ cm), during which time the nonlinear phase-shifting probe and signal fields must be present all the time. However, to acquire the same amount of nonlinear phase shift for the probe and signal waves in the present ARG system, the device transient time is only about 18 ps [35].

IV. DISCUSSION AND SUMMARY

Now we briefly discuss the Doppler effect due to the atom's thermal motion. Actually, our results can be readily generalized when an atom moves with a velocity V by the replacement $\delta_1 \to \omega_{21} - \omega_{P1} + k_{P1z}V_z$, $\delta_2 \to (\omega_{P1} - \omega_p) - \omega_{31} + (k_p - k_{P1})_z V_z = (\omega_{P1} - \omega_s) - \omega_{41} + (k_s - k_{P1})_z V_z$ (we assume all light fields propagate along the z direction, as suggested in the inset of Fig. 1). The V_z-dependent terms obtained are then averaged over a given thermal velocity distribution $f(V_z)$. From these discussions, we see that the velocity-dependent effect in the two-photon detunings δ_2 in the copropagating case $k_{P1}k_j > 0$ is much smaller than that in the counterpropagating case $k_{P1}k_j < 0$. Consequently, the velocity-dependent effect or the Doppler effect in the two-photon detunings can usually be neglected compared with that in the one-photon detuning if we choose the waves to propagate in the same direction. Moreover, such an effect in the one-photon detuning can also be efficiently suppressed if $\omega_{21} - \omega_{P1} \gg \omega_{P1z}V_z$, which is satisfied in our system.

The experimental demonstration of the phase gate requires the measurement of phase shifts, which will result in errors due to the fluctuations of light intensities and frequency detunings of the probe and signal fields. In order to minimize the effect of relative detuning fluctuations, one can take all lasers tightly phase-locked to each other. The light intensity with fluctuations of 1% will yield an error less than 2% in the phase measurement.

We should point out that although CPM is a very promising candidate for the design of deterministic optical quantum phase gates, it still faces some challenges. These include (i) how to achieve the sufficiently high single-photon intensity; (ii) how to overcome the phase noise induced by the noninstantaneous nonlinear response inherent in resonant atomic systems; and (iii) how to obtain a spatially homogeneous CPM necessary for effective entanglement between light pulses. These problems are now actively being investigated, and some methods for dealing with them have already been proposed [36]. On the other hand, in the present work we have treated the probe and signal fields in a classical way. Therefore, it would be easier to create the entanglement of macroscopic, coherent states rather than single-photon states. A full quantum treatment is still necessary but is beyond the scope of the present work.

To sum up, we have presented a scheme for obtaining entangled photons and quantum phase gates in a room-temperature four-state tripod-type atomic system with a two-mode ARG. We have analyzed the linear and nonlinear optical responses of the ARG system and shown that the scheme is fundamentally different from those based on EIT, and hence it can avoid significant probe-field absorption as well as a temperature-related Doppler effect. We have demonstrated that highly entangled photon pairs can be produced and rapidly responding polarization qubit quantum phase gates can be constructed based on the unique features of enhanced CPM and superluminal probe-field propagation of the ARG system. The method provided here can also be extended to study multiway entanglement and multiqubit phase gates.

ACKNOWLEDGMENTS

The authors thank Y. Li and L. Deng for useful discussions and suggestions. This work was supported by the NSF of China under Grants No. 10434060 and No. 10874043 and by the Key Development Program for Basic Research of China under Grants No. 2005CB724508 and No. 2006CB921104. CH was supported by the Fundação para a Ciência e a Tecnologia (FCT) under Grant No. SFRH/BPD/36385/2007 and the Calouste Gulbenkian Foundation 2009.

[1] M. A. Nielsen and I. L. Chuang, *Quantum Computation and Quantum Information* (Cambridge University Press, Cambridge, England, 2000).
[2] M. Fleischhauer, A. Imamoglu, and J. P. Marangos, Rev. Mod. Phys. **77**, 633 (2005), and references therein.
[3] K. Hammerer, A. S. Sorensen, and E. S. Polzik, Rev. Mod. Phys. **82**, 1041 (2010), and references therein.
[4] A. I. Lvovsky, B. C. Sanders, and W. Tittel, Nat. Photon. **3**, 706 (2009), and references therein.
[5] R. Santra, E. Arimondo, T. Ido, C. H. Greene, and J. Ye, Phys. Rev. Lett. **94**, 173002 (2005).
[6] T. Zanon-Willette, A. D. Ludlow, S. Blatt, M. M. Boyd, E. Arimondo, and J. Ye, Phys. Rev. Lett. **97**, 233001 (2006).
[7] T. Hong, C. Cramer, W. Nagourney, and E. N. Fortson, Phys. Rev. Lett. **94**, 050801 (2005).
[8] Y. Wu and L. Deng, Phys. Rev. Lett. **93**, 143904 (2004).
[9] G. Huang, L. Deng, and M. G. Payne, Phys. Rev. E **72**, 016617 (2005).
[10] H. Michinel, M. J. Paz-Alonso, and V. M. Pérez-García, Phys. Rev. Lett. **96**, 023903 (2006).
[11] C. Hang, V. V. Konotop, and G. Huang, Phys. Rev. A **79**, 033826 (2009).
[12] M. D. Lukin and A. Imamoğlu, Phys. Rev. Lett. **84**, 1419 (2000).
[13] A. Peng, M. Johnsson, W. P. Bowen, P. K. Lam, H.-A. Bachor, and J. J. Hope, Phys. Rev. A **71**, 033809 (2005).
[14] I. Friedler, D. Petrosyan, M. Fleischhauer, and G. Kurizki, Phys. Rev. A **72**, 043803 (2005).
[15] C. Ottaviani, D. Vitali, M. Artoni, F. Cataliotti, and P. Tombesi, Phys. Rev. Lett. **90**, 197902 (2003).
[16] S. Rebić, D. Vitali, C. Ottaviani, P. Tombesi, M. Artoni, F. Cataliotti, and R. Corbalán, Phys. Rev. A **70**, 032317 (2004).
[17] A. Joshi and M. Xiao, Phys. Rev. A **72**, 062319 (2005).
[18] C. Hang, Y. Li, L. Ma, and G. Huang, Phys. Rev. A **74**, 012319 (2006).
[19] If the group velocity of a light pulse is reduced by a factor of F from the speed of light in vacuum, the phase-shift operation will be a factor of F slower [26].
[20] R. Y. Chiao, Phys. Rev. A **48**, R34 (1993).
[21] A. M. Steinberg and R. Y. Chiao, Phys. Rev. A **49**, 2071 (1994).

[22] L. J. Wang, A. Kuzmich, and P. Pogariu, Nature (London) **406**, 277 (2000).
[23] M. D. Stenner, D. J. Gauthier, and M. A. Neifield, Nature (London) **425**, 695 (2003).
[24] G. S. Agarwal and S. Dasgupta, Phys. Rev. A **70**, 023802 (2004).
[25] K. J. Jiang, L. Deng, and M. G. Payne, Phys. Rev. A **76**, 033819 (2007).
[26] L. Deng and M. G. Payne, Phys. Rev. Lett. **98**, 253902 (2007).
[27] K. J. Jiang, L. Deng, E. W. Hagley, and M. G. Payne, Phys. Rev. A **77**, 045804 (2008).
[28] G. Huang, C. Hang, and L. Deng, Phys. Rev. A **77**, 011803(R) (2008).
[29] C. Hang and G. Huang, Opt. Express **18**, 2952 (2010).
[30] R. W. Boyd and D. J. Gauthier, Science **326**, 1077 (2009).
[31] Due to the symmetric configuration of the system, the linear and nonlinear susceptibilities of both the probe and signal fields are almost equal [see Eq. (5)]. Hence, the curves plotted in Fig. 3 are valid for both the probe and signal fields.
[32] Q. A. Turchette, C. J. Hood, W. Lange, H. Mabuchi, and H. J. Kimble, Phys. Rev. Lett. **75**, 4710 (1995).
[33] V. Coffman, J. Kundu, and W. K. Wootters, Phys. Rev. A **61**, 052306 (2000).
[34] M. Bajcsy, S. Hofferberth, V. Balic, T. Peyronel, M. Hafezi, A. S. Zibrov, V. Vuletic, and M. D. Lukin, Phys. Rev. Lett. **102**, 203902 (2009).
[35] The lead time is typically about 10% of c. Thus the device transient time can be estimated quite accurately by using the free-space speed of light [27].
[36] K.-P. Marzlin, Z.-B. Wang, S. A. Moiseev, and B. C. Sanders, J. Opt. Soc. B **27**, A36 (2010).